Silylation of bacterial cellulose to design membranes with intrinsic anti-bacterial properties

Guillaume Chantereau, Nettie Brown, Marie-Anne A Dourges, Carmen S.R. Freire, Armando J.D. Silvestre, Gilles Sèbe, Véronique Coma

Silylation of bacterial cellulose to design membranes with intrinsic anti-bacterial properties

Guillaume Chantereau[a,b], Nettie Brown[c], Marie-Anne Dourges[d], Carmen S. R. Freire[b], Armando J. D. Silvestre[b], Gilles Sebe[a*], Véronique Coma[a,*]

[a] University of Bordeaux, LCPO, UMR 5629, F-33600 Pessac, France

[b] CICECO – Aveiro Institute of Materials, Department of Chemistry, University of Aveiro, 3810-193 Portugal

[c] University of Georgia, Biomedical Engineering, Athens, GA 30602, United States

[d] University of Bordeaux, Institut des Sciences Moléculaires, UMR-CNRS 5255, F-33405 Talence, France

[*]**Corresponding authors:** veronique.coma@enscbp.fr (Véronique Coma) and gilles.sebe@enscbp.fr (Gilles Sèbe)

Email addresses: guillaumechantereau@gmail.com (Guillaume Chantereau), nettiebrown10@uga.edu (Nettie Brown), marie-anne.dourges@u-bordeaux.fr (Marie-anne Dourges), cfreire@ua.pt (Carmen S. R. Freire), armsil@ua.pt (Armando J.D. Silvestre),

Abstract

In this work, we report a convenient method of grafting non-leachable bioactive amine functions onto the surface of bacterial cellulose (BC) nanofibrils, via a simple silylation treatment in water. Two different silylation protocols, involving different solvents and post-treatments were envisaged and compared, using 3-aminopropyl-trimethoxysilane (APS) and (2-aminoethyl)-3-aminopropyl-trimethoxysilane (AEAPS) as silylating agents. In aqueous

and controlled conditions, water-leaching resistant amino functions could be successfully introduced into BC, via a simple freeze-drying process. The silylated material remained highly porous, hygroscopic and displayed sufficient thermal stability to support the sterilization treatments generally required in medical applications. The impact of the silylation treatment on the intrinsic anti-bacterial properties of BC was investigated against the growth of *Escherichia coli* and *Staphylococcus aureus*. The results obtained after the *in vitro* studies revealed a significant growth reduction of *S. aureus* within the material.

Keywords: bacterial cellulose, nanocellulose, aminosilane, anti-bacterial, silylation

1. Introduction

In recent years, the field of biomedical materials has witnessed rapid progress, increasingly calling upon the use of efficient sustainable based materials, as cellulose based materials, in applications such as wound healing, drug delivery systems, vascular grafts or scaffolds for *in vivo* tissue engineering (Agarwal, McAnulty, Schurr, Murphy, & Abbott, 2011; Jorfi & Foster, 2015). This biopolymer is particularly interesting because of its renewability, biodegradability, and biocompatibility; however, it is not endowed with antibacterial activity, one of the most desired properties in the medical field (O'Neill, 2014). To address this issue, anti-bacterial systems based on cellulose mixed with bioactive compounds have been proposed, such as those with silver nanoparticles (Berndt, Wesarg, Wiegand, Kralisch, & Müller, 2013) or anti-bacterial peptides (Nguyen, Gidley, & Dykes, 2008). However, numerous problems may result from the uncontrolled release of bioactive agents, such as the development of multi-resistant micro-organisms (Lewis, 2001; O'Neill, 2014). As a consequence, antibiotic-resistant bacterial strains such as *Staphylococcus aureus* (Boswihi & Udo, 2018) or *Escherichia coli* (Milović, Wang, Lewis, & Klibanov, 2005) are now spreading in the environment and becoming one of the greatest health threats of this

48 century (O'Neill, 2014). To circumvent this problem, the immobilization of bioactive agents
49 by chemical bonding offers the opportunity to produce materials, which release no deleterious
50 chemicals and are able to promote bioactivity by simple contact. Until now, essentially
51 materials grafted with active ammonium moieties have been proposed, such as glass grafted
52 with quaternized polyethylenimine (Milović et al., 2005), microcrystalline cellulose grafted
53 with comb-like N,N-dimethyldodecylammonium groups (Bieser, Thomann, & Tiller, 2011) or
54 chitosan grafted with nisin in acidic conditions (X. Zhu et al., 2015). The mechanism of action
55 of these systems is still unclear, but is thought to be related to the positive charge of the
56 ammonium functions, which supposedly interacts with the negative charges at the microbial
57 cell surface (phospholipids), leading to a modification of the membrane permeability and
58 leakage of intracellular components (Bieser & Tiller, 2011; Fernandes et al., 2014; Helander,
59 Nurmiaho-Lassila, Ahvenainen, Rhoades, & Roller, 2001).
60 Among the cellulose materials with high potential in the biomedical field, bacterial
61 cellulose (BC) is particularly attractive as it naturally displays various properties required for
62 biomedical applications, namely: high water-holding capacity, good mechanical properties,
63 biocompatibility and non-toxicity (Agarwal et al., 2011; Czaja, Young, Kawecki, & Brown,
64 2007). BC is an extracellular polysaccharide produced by the bacteria of the genus
65 *Gluconacetobacter*, *Rhizonium*, *Sarcina*, *Agrobacterium* or *Alcaligenes* (Berlioz, 2007;
66 Chawla, Bajaj, Survase, & Singhal, 2009; Esa, Tasirin, & Rahman, 2014), which has already
67 proved its efficiency as a wound healing membrane (Fontana et al., n.d.; US10425978, 2003),
68 arterial substitute (Wippermann et al., 2009), or matrix for transdermal drug delivery systems
69 (Silva, Rodrigues, et al., 2014; Trovatti et al., 2011). To prepare BC with anti-bacterial
70 activity, the grafting of ammonium moieties by reaction with (3-aminopropyl)-
71 trimethoxysilane (APS) has been proposed as a method to impart anti-bacterial properties to
72 the material (Fernandes et al., 2013; Saini, Belgacem, Salon, & Bras, 2016; Shao et al., 2017;

Taokaew, Phisalaphong, & Newby, 2015). Interesting results have been obtained, but it is not clear at this stage if the anti-bacterial activity observed in these pioneering works resulted from a contact mechanism or from the release of the amino moieties after hydrolysis of the grafted silane. It has indeed been reported that such grafting is generally unstable in the presence of water, as the pendant amino group can catalyze the hydrolysis of the chemical bonds formed between APS and the hydroxylated substrate (Etienne & Walcarius, 2003; Smith & Chen, 2008; M. Zhu, Lerum, & Chen, 2012).

In this context, we report here a thorough investigation of the functionalization of BC with two different aminosilanes, APS and (2-aminoethyl)-3-aminopropyl-trimethoxysilane (AEAPS), with the objective of producing a water-stable material with intrinsic anti-bacterial activity. Two different silylation protocols, involving different solvents (acetone or water) and post-treatments (with or without heat curing), were envisaged and compared. The stability of the silane grafting after prolonged soaking in water was investigated in detail. The thermal properties and ultrastructure of the materials with the highest level of non-leachable silane were subsequently characterized by TGA, SEM and porosimetry. Finally, the impact of the silylation treatment on the anti-bacterial activity by contact against the growth of two target bacteria, *E. coli (*Gram-negative) and *S. aureus* (Gram-positive), was investigated and discussed.

2. Experimental

2.1. Materials

(3-Aminopropyl)-trimethoxysilane (APS) was purchased from TCI and (2-aminoethyl)-3-aminopropyl-trimethoxysilane (AEAPS) from Gelest Inc. Tryptose broth was bought from Difco Laboratories and bacteriological agar A1010HA was provided by Biokar Diagnostics. Sodium chloride was obtained from Sigma Aldrich and hydrochloric acid 37% from Fisher

Scientific. All chemicals were used without purification. Distilled water Milli-Q Direct 8 (Millipore) was used in all experiments. All other reagents used were of analytical grade.

2.2. Preparation of BC

Bacterial cellulose membranes were produced using *Gluconacetobacter sacchari* strain (Silva, Drumond, et al., 2014) in conventional culture media conditions (Hestrin & Schramm, 1954). Briefly, a subculture was incubated at 30°C for 48h, in static conditions. The flask was then vigorously agitated and 5 mL of the culture media added to 45 mL HS medium in 250 mL Erlenmeyer flasks. The production of BC was carried out under sterile conditions. The flasks were incubated at 30°C, in a static incubator, for 96h. BC membranes were then treated three times with 0.5 M NaOH solution at 90°C for 30 min in order to eliminate attached cells. Next, the membranes were washed with water to remove components of the culture media and other residues. This step was repeated until pH reached neutral value. Wet BC membranes were stored in water at 4°C until use.

2.3. Preparation of silylated BC

2.3.1. Silylation in acetone (Protocol 1)

This protocol was inspired by the work of Fernandes et al., 2013 (Fernandes et al., 2013). 5 g of wet BC membranes (about 30-40 mg of dry content) were subjected to solvent exchange in acetone for 1h under stirring (repeated 6 times). Membranes were then placed between two paper sheets and pressed at 39 kPa for 2 min, in order to remove part of the absorbed acetone (between 50 and 70 wt% of acetone removal). 1 ml of a 340 mmol/L APS or AEAPS solution (in acetone) was then deposited on top of the BC membranes, to reach an anhydroglucose/silane molar ratio of 1:1. The material was left for 2h at room temperature, until complete absorption of the aminosilane solution by the substrate. Samples were subsequently dried at room temperature and pressed overnight at 39 kPa (between two paper

sheets). Finally, the obtained transparent films were cured at 120°C for 2h. Samples were stored in a desiccator containing phosphorous pentoxide at least 24h before characterization. Samples were named according to the type of silane and concentration used in the process (BC-APS_{340} or BC-$AEAPS_{340}$).

2.3.2. Silylation in water (Protocol 2)

This protocol was inspired by the work of Zhang *et al.*, 2014 (Zhang, Sèbe, Rentsch, Zimmermann, & Tingaut, 2014). Two types of experiments were performed based on this method, starting from 5g of wet BC membrane (about 30 mg of dry content). In the first set of experiments (Protocol 2a), BC membranes were freeze-dried prior to functionalization, while in the second set (Protocol 2b), the membranes were used in their wet form, after removal of 50 to 70% of the water under pressure (same method as in Protocol 1).

In both cases, 340 mmol/L (or 280 mmol/L) of an APS or AEAPS water solution (acidified with HCl/ pH = 4.6) was deposited on top of a dry or wet BC membrane, to reach an anhydroglucose/silane molar ratio of 1:1 (or 1:0.75). The material was left for 2h at room temperature until complete absorption of the aminosilane solution by the substrates. Finally, the membranes were soaked in liquid nitrogen and freeze-dried for 24h. Samples were stored in a desiccator with phosphorous pentoxide at least 24h before characterization. Samples were named according to the type of silane and concentration used in the process (BC-APS_{340}, BC-$AEAPS_{340}$ or BC-$AEAPS_{280}$).

2.4. Leaching experiments

Silylated BC samples were soaked in water at room temperature for 20h. After freeze-drying, the samples were stored in a desiccator containing phosphorous pentoxide for at least 24h before characterization. The stability of the grafting was assessed by comparing the infrared spectra and nitrogen content in the samples, before and after leaching.

2.5. *Characterization of unmodified and silylated BC*

2.5.1. Fourier transform infrared spectroscopy (FT-IR)

FT-IR spectra were recorded between 400 and 4000 cm^{-1} at a resolution of 4 cm^{-1} (32 scans), using a Nicolet FT-IR spectrometer (AVATAR 370) in transmission mode. 2 mg of samples were ground and mixed with 200 mg of KBr to prepare pellets. For comparison purposes, spectra were adjusted with the same baseline correction (polynomial with 1 iteration and 6 points at 3800, 2280, 1900, 1262, 876 and 411 cm^{-1}) and were normalized to the $\delta_{as}(CH_2)$ asymmetric bending of cellulose at 1430 cm^{-1} (not affected by the chemical modification).

2.5.2. Size exclusion chromatography (SEC)

SEC analysis was carried out on a Varian apparatus equipped with TosoHaas TSK gel columns and a differential refractometer detector. PBS pH 7.0 served as eluent, at a flow rate of 0.6 $mL.min^{-1}$, and calibration was achieved with pullulan/dextran standards.

2.5.3. Elemental analysis

Elemental analysis data were obtained from SGS Multilab. The atomic weight ratio of the nitrogen present in the silylated samples (N wt%) was measured according to protocol ASTM D5373 ("ASTM D5373-16, Standard Test Methods for Determination of Carbon, Hydrogen and Nitrogen in Analysis Samples of Coal and Carbon in Analysis Samples of Coal and Coke," 2016). Experiments were conducted in duplicate and results were averaged. The silane content within the material was estimated from N wt%, based on the molecular weight of the monomer unit of the condensed polysiloxane obtained after hydrolysis and condensation of the aminosilane, namely $SiO_{3/2}CH_2CH_2CH_2NH_2$ for APS (M =109.49 $g.mol^{-1}$) and $SiO_{3/2}CH_2CH_2CH_2NHCH_2CH_2NH_2$ for AEAPS (M = 147.52 $g.mol^{-1}$). N% was also used to estimate the amine content, in mmol per gram of silylated BC.

2.5.4. Thermogravimetric analyses

Thermogravimetric analyses were performed under air, with a TGA-Q500 system from TA instruments operated at a heating rate of 10°C.min^{-1}. The residual water content was quantified by measuring the weight loss in the thermo-oxidative curves at 150°C. The 5% weight loss temperature ($T_{5\%}$) was estimated based on the degradation of the dry cellulosic material (i.e. excluding the loss due to water vaporization). The temperature of maximum rate of degradation (T_m) was determined from the maximum of the derivative TG curves. The char yield at 750°C was calculated in terms of weight percentage of dry material.

2.5.5. Water absorption assessment

The water absorption capacity of the unmodified and silylated BC materials, expressed as g of water/g of dry material, was evaluated by soaking the samples in 50 mL water, and gravimetrically measuring the amount of water absorbed after 72h. The values of four replicates were averaged in each experiment and the standard deviation was calculated.

2.5.6. Scanning electron microscopy

Scanning electron microscopy (SEM) was performed on a QUANTA 200 microscope from FEI. The voltage was set at 5 kV, in 50 Pa low vacuum atmosphere. Samples for cross-section imaging were prepared by breaking membranes after freezing in liquid nitrogen. Samples were placed on a conducting tape without coating.

2.5.7. Porosimetry and density

The porosity and density of the BC samples were evaluated by mercury intrusion porosimetry, with a Micromeritics Autopore IV 9500 porosimeter, set with the following parameters: contact angle = 130°; mercury surface tension = 485 mN m^{-1}; maximum intrusion

192 pressure = 124 MPa. The Brunauer-Emmett-Teller (BET) specific surface area was measured
193 by nitrogen sorption, with a Micromeritics ASAP 2010.

194 2.5.8. *In vitro* antibacterial properties of silylated-BC

195 To evaluate BC anti-bacterial properties, membranes were specifically autoclaved at
196 120°C for 15 min and the synthesis of silylated BC and the leaching experiment, previously
197 described in sections 2.3 and 2.4, were performed in sterile conditions under a laminar flux
198 hood. To evaluate inherent anti-bacterial activity, and not activity due to the release of
199 aminosilane, BC and silylated BC produced by Protocol 2b were tested after the leaching
200 experiments.

201 In addition, in order to extensively protonate the amine groups of the silylated
202 membranes, chemically-modified BC membranes (10 mg) were soaked for 2h in 5mL of
203 hydrochloric acid solution (pH 2.07). As control materials, unmodified-BC membranes were
204 soaked for 2h in HCl in the same conditions as mentioned before (BC-HCl) or just soaked in 5
205 mL water for 2h (BC), mainly to determine the impact of the acid treatment. Subsequently,
206 membranes were washed three times with water and dried in a vacuum-oven at 60°C.
207 Anti-bacterial activity of BC, BC-HCl, BC-APS_{340}, BC-$AEAPS_{340}$ and BC-$AEAPS_{280}$
208 was tested against *E. coli* ATCC 25922 and *S. aureus* ATCC 6538. Overnight cultures in
209 tryptose or nutrient broth for *E. coli* and *S. aureus*, respectively, were centrifuged at 2500 rpm
210 for 8 min and the supernatant was removed and replaced by physiological water (9 $g.L^{-1}$
211 NaCl) to wash the inoculum. This step was repeated 3 times. Dilution was adjusted to place a
212 9 µL droplet of about 10^2 cells on top of 1 cm^2 material samples previously deposited on
213 tryptose or nutrient agar, depending on the target strain. Petri dishes were then stored at 4°C
214 for 4h to allow penetration of the inoculum through the sample in order to reach the agar
215 medium. After 14h of incubation at 30°C, the materials and the agar below were recovered,

immersed in 9 mL physiological water and vortexed for 30 s. Successive 10-fold dilutions in physiological water were made up to 10^4. For each dilution, 0.1 mL aliquots were removed and plated a tryptose or nutrient agar medium for *E. coli* and *S. aureus* numeration, respectively. The number of viable bacterial cells on each material was determined and the results were expressed in $\log_{10}(CFU/cm^2)$. The experiments were conducted in triplicate and results averaged.

3. Results and discussion

3.1. Silylation of BC with APS and AEAPS

In this study, anti-bacterial amino moieties were introduced into BC membranes using two different aminosilanes bearing one or two amine groups, *i.e.* (3-aminopropyl)-trimethoxysilane (APS) and (2-aminoethyl)-3-aminopropyl-trimethoxysilane (AEAPS), respectively. Silylation was performed by reacting BC with the trimethoxysilane functions according to two different protocols inspired by the literature (Protocols 1 & 2) and illustrated in Fig. 1. Irrespective of the protocol, the grafting involves three steps: i) hydrolysis of the alkoxysilanes into silanols, ii) homocondensation of the silanols into oligomers, and iii) condensation of the oligomers with the BC substrate (Fernandes et al., 2013; Zhang et al., 2014; Zhang, Tingaut, Rentsch, Zimmermann, & Sèbe, 2015). The main differences between the two protocols lie in the type of solvent used (acetone or water) and the procedure employed to condense the silanes (with or without heat curing). The water required for the hydrolysis of the aminosilanes in Protocol 1 is provided by a layer of adsorbed water at the surface of the BC nanofibrils, while the condensation with BC is initiated by a heating step at 120°C (Fernandes et al., 2013). With Protocol 2, the silanes are readily hydrolyzed and homocondensed in the form of oligomers (silane sol) before contact with BC. The subsequent condensation with BC takes place at a low temperature, when the water solvent is

progressively removed from the medium by freeze-drying (Zhang et al., 2014, 2015). Whatever the protocol used, the stability of the grafting was probed by performing a leaching test in water (the silylated samples were soaked in water for 20 h).

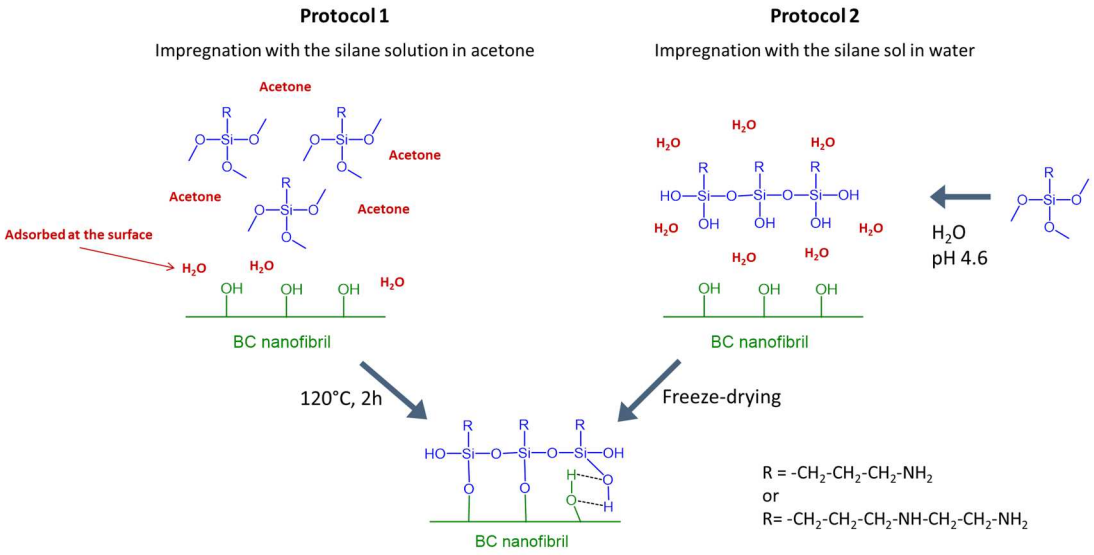

Fig. 1. Reaction schemes of the two protocols used for the silylation of BC with APS and AEAPS.

A first set of experiments was performed following the procedure of Fernandes *et al.* in acetone (Protocol 1) (Fernandes et al., 2013). The presence of silane moieties in the modified samples (BC-APS$_{340}$) was confirmed by measuring nitrogen content by elemental analysis (Table 1), and observing the δ(NH) amine vibration in the 1600-1590 cm^{-1} region of the FT-IR spectrum (Fig. 2, Protocol 1). The silane content was estimated from the nitrogen content, as described in the experimental section.

The δ(NH) band disappeared after the leaching test in water (Fig. 2, Protocol 1), with about 80 wt% of the silane being removed (Table 1), indicating that the grafting was not stable in this aqueous environment. This instability could result from the hydrolysis of the Si-O-C bonds catalyzed by the amine groups, through the formation of five-membered cyclic intermediates, as was reported for silica particles grafted with APS (Etienne & Walcarius, 2003; Smith & Chen, 2008; M. Zhu et al., 2012). To circumvent this problem, Zhu *et al.*

(2012) suggested increasing the chain length separating the silicon atom from the primary amine moiety, using AEAPS as a silylating agent. This structure prevents the formation of five-membered cyclic intermediates, leading to significant improvement in the stability of the grafted silane in their case. We therefore envisaged silylating our BC membrane with AEAPS, using the same molar concentration as with APS (Table 1 and Fig. 2). Using AEAPS instead of APS led to a significant improvement in silane grafting, probably because the high molecular weight AEAPS was vaporized less during the heating step at 120°C. The δ(NH) vibrations of the primary and secondary amine functions of AEAPS were identified in the same FT-IR region as for APS (Fig. 2), however, contrary to expectations, the silylated material still lost about 80 wt% of the silane after the leaching test in water. In view of these results, we inferred that the AEAPS molecules may have been poorly condensed with the cellulose substrate in our experimental conditions. Nevertheless, a significantly higher amount of non-leachable amine groups was grafted within the BC material when AEAPS was used (about seven times more than with APS), both because more silane was introduced initially, and because each monomer contained two amine functions.

Table 1

Amount of nitrogen (wt%), silane (wt%) and amine functions (mmol/g) within the silylated BC materials before and after water leaching (determined by elemental analysis).

		Protocol 1		**Protocol 2a**		**Protocol 2b**	
Leaching experiment		***Before***	***After***	***Before***	***After***	***Before***	***After***
BC-APS$_{340}$	**N(wt%)**	1.3	0.3	4.0	0.5	4.3	0.7
	Silane (wt%)	9.9	2.2	31.4	3.6	33.6	5.9
	Amine (mmol/g)	0.9	0.2	2.9	0.3	3.1	0.5
BC-AEAPS$_{340}$	**N(wt%)**	5.8	1.0	5.0	1.0	5.9	2.63
	Silane (wt%)	30.6	5.0	26.4	5.2	31.0	13.8
	Amine (mmol/g)	8.3	1.4	7.2	1.4	8.4	3.8
BC-AEAPS$_{280}$	**N(wt%)**					4.6	3.4
	Silane (wt%)					24.3	18.2
	Amine (mmol/g)					6.6	4.9

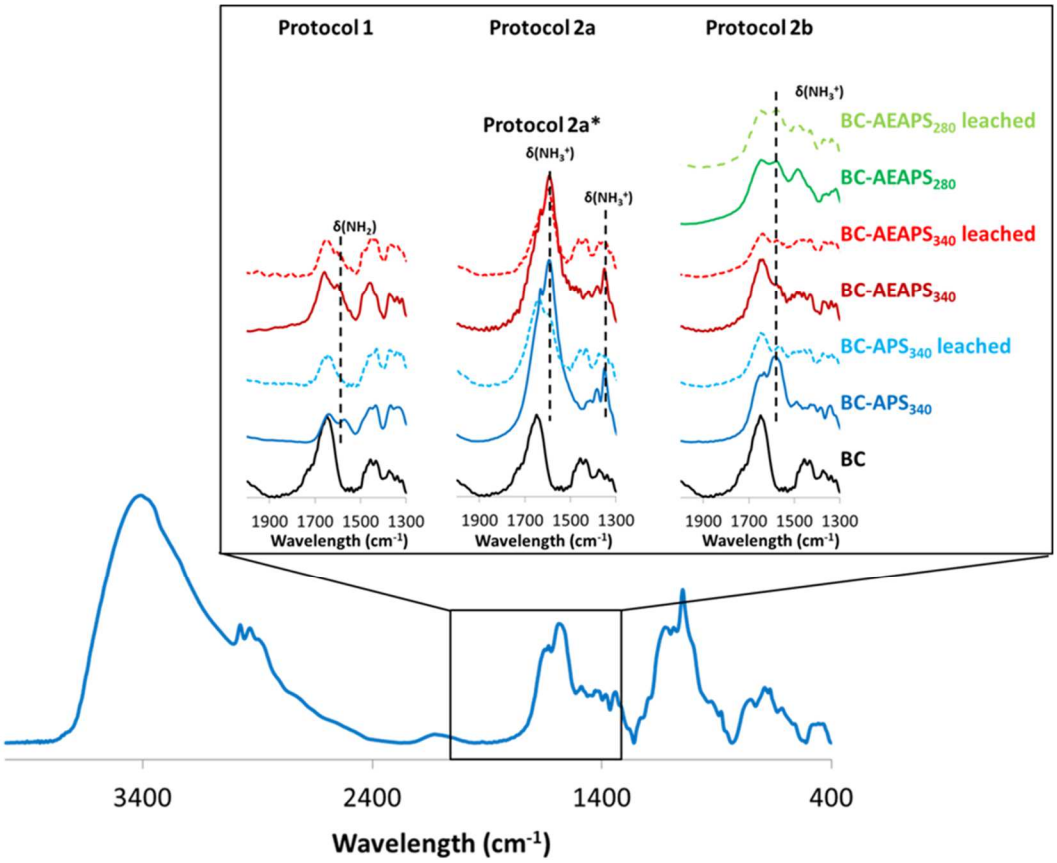

277

278 **Fig. 2.** FT-IR spectra in the 2000-1300 cm^{-1} region of unmodified BC, BC-APS_{340} before and after
279 water leaching, BC-$AEAPS_{340}$ before and after water leaching and BC-$AEAPS_{280}$ before and after
280 water leaching.

281 In an alternative approach, we envisaged silylating the BC membranes (with both APS
282 and AEAPS) following the procedure of Zhang *et al.* (Protocol 2), who reported a simple
283 method to graft alkoxysilane molecules onto the surface of nanofibrillated cellulose in water
284 medium (Fig. 1) (Zhang et al., 2015). A first set of experiments was performed starting from
285 freeze-dried BC (Protocol 2a), in order to control the silane/BC and silane/water ratios during
286 the treatment. Before being introduced into the BC network, the aminosilanes were
287 hydrolyzed at pH 4.6, leading to a silane sol composed of polysiloxane oligomers, which were
288 analyzed by SEC in the case of APS (Fig. S1 of supporting information). Results indicated
289 that the APS sol was composed mostly of a mixture of two oligomers, with average molecular
290 weights of 1391 g/mol (10-15 condensed units) and 5108 g/mol (35-60 condensed units).

After the treatment, the amount of nitrogen in BC was again evaluated by elemental analysis (Table 1, Protocol 2a) and the presence of silane was confirmed by FT-IR spectroscopy (Fig. 2, Protocol 2a). The FT-IR spectra displayed stronger absorption bands in the 1600-1500 cm^{-1} and 1350 cm^{-1} regions compared with protocol 1, which could be related to the presence of bicarbonate salts, possibly formed after contact between the grafted NH_2 groups and atmospheric CO_2 (Culler, Naviroj, Ishida, & Koenig, 1983). The infrared vibrations of these salts are indeed expected in the same region. Compared with the treatment in acetone, the Protocol 2a in water allows a greater amount of APS to be grafted (about three times more in Table 1), probably because the vaporization of APS was prevented in that case, as the sample was not heated during the process. In addition, no significant difference in grafting level was noted between the two protocols when the higher molecular weight AEAPS was used. Here again, a significant amount of silane was leached out after prolonged contact with water (~ 90 wt% with APS and ~ 80 wt% with AEAPS), suggesting once again that the silane oligomers were poorly condensed with the cellulose substrate, and/or were partly hydrolyzed in the presence of water. We reasoned at this stage that the use of dry BC might have reduced the efficiency of the treatment when the silane sol was deposited at the surface of this highly hygroscopic substrate. Indeed, the water surrounding the silane oligomers is expected to be absorbed within seconds after contact with the dry cellulosic substrate. As a result, the homocondensation of the oligomers at the surface of the film should be highly favored, thereby preventing their in-depth penetration into the BC network, and limiting the possibility for condensation with the bulk cellulose fibrils. To address this problem, the previous experiments were reproduced, but this time starting from never-dried BC (Protocol 2b). The elemental analysis and FT-IR data obtained with Protocol 2b are reported in Table 1 and Fig. 2, respectively. The silylation levels obtained with wet BC were not significantly different from those obtained with Protocol 2a (Table 1), yet the intensity of the δ(NH) vibrations in

316 the FT-IR spectra was lower, presumably because fewer bicarbonate salts were formed by
317 contact with CO_2. Compared with Protocol 2a, the resistance to water leaching was
318 significantly improved when AEAPS was used. About 55 wt% of the silane was lost after
319 prolonged contact with water in that case, instead of the 80 wt% loss previously noted with
320 dry BC. The BC grafted with APS was also more resistant to water leaching, but to a much
321 lower extent (loss of ~ 80 wt% silane instead of ~ 90 wt%). The better stability obtained with
322 AEAPS was attributed to the structure of AEAPS, which prevents the amine-catalyzed
323 hydrolysis generally noted with APS (Zhu *et al.* 2012). In an attempt to further limit the
324 homocondensation of the hydrolyzed silane, i.e. further promote its condensation with the
325 cellulosic scaffold, an additional sample was silylated with a lower concentration of AEAPS
326 (BC-$AEAPS_{280}$ in Table 1). As expected, the resistance to water leaching was further
327 increased using this strategy, only 25% wt% of the silane introduced initially being now
328 leached out after 20h in water.

329 In view of the encouraging results obtained with Protocol 2b, only the silylated
330 samples obtained in these conditions were selected for further investigations. In addition, only
331 the water-leached samples, i.e. those containing only non-leachable silanes, were thoroughly
332 characterized.

333 *3.2. Thermal properties of silylated BC*

334 The TGA thermograms under air flow of the unmodified and water-leached silylated
335 samples (Protocol 2b) are presented in Fig. S2 of supporting information, and the degradation
336 data are summarized in Table 2. The amount of residual water adsorbed by the dry material
337 was evaluated from the weight loss at 150°C, and is also reported in Table 2. The thermogram
338 of unmodified BC is consistent with the thermal behavior generally observed for bacterial
339 cellulose (Cheng, Catchmark, & Demirci, 2009; Fernandes et al., 2013). The introduction of
340 amine moieties into BC led to an increase in the hygroscopic character of the material, the

water content increasing concomitantly with the nitrogen content. No significant modification of the thermal stability of the material was noted after the APS treatment, but samples treated with AEAPS displayed a 5 % lower weight loss temperature ($T_{5\%}$), while the temperature of maximum rate of degradation (T_m) was only slightly modified. The reduced $T_{5\%}$ noted with AEAPS could result from the release of volatile compounds, by cleavage of the AEAPS moieties between 200 and 240°C (through nucleophile reactions initiated by the terminal amine group for instance). The solid residue at 750°C obtained after degradation of the silylated samples (Table 2), was assigned to silicon inorganic species formed at high temperature (SiO_2). In any case, the silylated materials displayed sufficient thermal stability to support the sterilization treatments generally required in the medical applications targeted.

Table 2

TGA data obtained after analysis under air flow of BC, BC-APS_{340}, BC-$AEAPS_{340}$ and BC-$AEAPS_{280}$, produced according to Protocol 2b (water-leached samples). Water and amine content are also reported.

	$T_{5\%}$ (°C)	T_{max} (°C)	Residue at 750 °C (%)	Water content (%)	Amine content (mmol/g)
BC	288	327	1.7	1.5	0
BC-APS_{340}	284	329	5.1	3.6	0.5
BC-$AEAPS_{340}$	207	320	17.1	9.9	3.8
BC-$AEAPS_{280}$	238	333	18.0	7.1	4.9

3.3. Ultrastructure

The cross-sections of the freeze-dried unmodified and silylated samples were examined by SEM (Fig. 3). Irrespective of the treatment, the fibrillar structure of the BC material was preserved after silylation. All samples consisted of a 3D network of nanofibrils of varying diameters (∅ = 10 to 200 nm) forming a porous structure. The porosity and density of the freeze-dried samples were evaluated by mercury intrusion porosimetry, while the BET

specific surface area was determined by nitrogen sorption (Table 3 and Fig. S3 of supporting information).

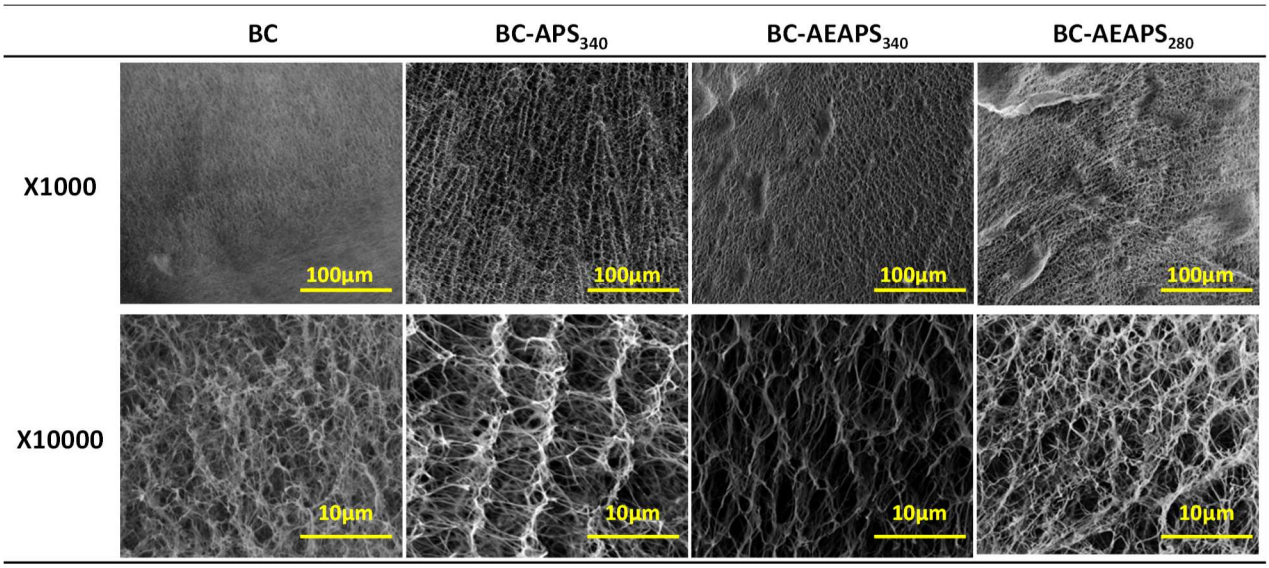

Fig. 3. SEM micrographs of the cross-sections of unmodified and water-leached silylated samples. Two magnifications are shown with scale bars of 100 and 10 µm.

The silylation treatment did not significantly modify the porosity of the samples, which remained relatively high for both BC-AEAPS$_{340}$ and BC-AEAPS$_{280}$. Therefore, the presence of silane during the freeze-drying step did not significantly modify the structure of the membrane. However, the BET surface area decreased significantly after silylation, which can be partly attributed to the fact that 1 g of BC-AEAPS$_{340}$ or BC-AEAPS$_{280}$ contained only 0.69 g or 0.74 g of cellulosic material, respectively (Table 1). Hence, the BET surface area per gram of cellulose should be closer to 67 and 65 %, respectively. The difference still noted compared with the unmodified sample can then be reasonably attributed to a thickening of the cellulosic scaffold after condensation of the silane at the surface of the BC nanofibrils (a coarser structure is generally observed with silylated samples in Fig. 3). In all cases, the nitrogen adsorption isotherms of the samples, Fig. S3 of supporting information, displayed a type II profile, characteristic of a macro-porosity (> 50 nm) with no micro-pores (< 2 nm) (Thommes et al., 2015). The increase in density noted with the silylated samples, was

attributed to a compression of the specimen during the mercury intrusion experiments (clearly observed in the case of the BC-AEAPS$_{340}$ sample). Therefore, pore size distribution was not evaluated with this technique, as it would probably vary during measurements. Although the BC material was more hygroscopic after silylation (Table 2), its water absorption capacity was reduced (Table 3), which can again be attributed to the fact than the cellulose content in 1 g of silylated material is less than in 1 g of unmodified BC. The water absorption capacity of the silylated BC scaffold nevertheless remained high.

Table 3

Density, porosity, specific surface area and water absorption capacity of the unmodified and water-leached silylated samples.

	Mercury intrusion data		Nitrogen data	Water abs. ass. data
	Density (kg/m^3)	Porosity (%)	BET surface area (m^2/g)	Absorbed water (g H_2O / g dry material)
BC	11	95	87	82
BC-AEAPS$_{340}$	28	92	52	37
BC-AEAPS$_{280}$	15	96	46	49

3.4. Anti-bacterial properties of silylated-BC

Antibacterial activities of the silylated-BC were first assessed by the plate-counting method against *E. coli* and *S. aureus* as the gram-negative and gram-positive model strains, respectively (Table 4).

For *E. coli,* BC and BC-HCl resulted in similar bacterial growth, around 9.0 $\log_{10}$(CFU/cm²). This showed that the possible residual acid after BC HCl-treatment did not lead to bacterial inhibition. Silylated BC without the protonation step in acidic conditions did not show any bacterial inhibition compared to the BC control. After HCl-treatment, silylated BC reduced the *E. coli* to 8.5, 8.1 and 7.9 $\log_{10}$(CFU/cm²) for BC-APS$_{340}$, BC-AEAPS$_{340}$ and BC-AEAPS$_{280}$, respectively, but unfortunately at a very low level. The commonly accepted

mode of action of anti-bacterial activity of amino groups is related to the positive charge of the corresponding ammonium functions (Bieser & Tiller, 2011; Fernandes et al., 2014; Helander et al., 2001). Thanks to elemental analysis, the number of moles of primary amines in BC-APS_{340}, BC-$AEAPS_{340}$ and BC-$AEAPS_{280}$ membranes after leaching experiments is known. The APS solution had pH values of 10.16 (in water) and 2.23 (in HCl) and the AEAPS solution had pH values of 10.08 (in water) and 6.80 (in HCl). Knowing the pKa of free APS (9.6) and AEAPS (9.3), without HCl treatment, only 21.6% of amine functions are protonated with APS and 14.2% with AEAPS, while the protonation is higher than 99.6% for both APS and AEAPS treated by the HCl solution. Thus, contrary to what was expected, the selected *E. coli* strain showed low sensitivity to chemically modified-BC, even after the protonation step.

Compared to *E. coli*, *S. aureus* demonstrated high sensitivity to silylated-BC. First, BC and BC-HCl showed similar behavior and reached about 10 $\log_{10}$(CFU/cm²) within 14 days of incubation. On BC-APS_{340}, BC-$AEAPS_{340}$ and BC-$AEAPS_{280}$ previously treated by HCl, the viable cell charges after incubation were 9.8, 7.0 and 6.3 $\log_{10}$(CFU/cm²), respectively. As has been frequently observed with various active agents or materials, silylated-BC showed much greater efficacy against the gram-positive pathogen than the gram-negative one. This could be due to differences in the outer cell walls and membranes of gram-negative and gram-positive bacteria. Gram-negative bacteria have a hydrophilic outer membrane and degradative and detoxifying enzymes in the periplasmic space (Beveridge, 1999), while Gram-positive bacteria do not have an outer membrane or periplasmic space containing protective enzymes (Beveridge, 1999; Shan, Cai, Brooks, & Corke, 2007).

In addition, by contrast with *E. coli*, a strong difference was observed between APS-containing BC (no significant log reduction compared to controls) and AEAPS-containing BC (3 to 4.0 log reduction compared to controls). In addition to the variable aminosilane

concentration, this could be due to the longer distance between the cellulosic backbone and the ammonium groups in BC-AEAPS. Indeed, Bieser *et al.* suggested that different mechanisms can allow bioactivity by contact, depending on the side-chain length (Bieser & Tiller, 2011).

Table 4

Number of *E. coli* and *S. aureus* colonies in the BC-materials in $\log_{10}$(CFU/cm²) after 14h incubation. Experiments were conducted in triplicate and results averaged.

	E. coli		*S. aureus*	
	Untreated	**HCl treatment**	**Untreated**	**HCl treatment**
BC	8.92 ± 0.08	9.07 ± 0.06	10.34 ± 0.12	10.29 ± 0.10
BC-APS$_{340}$	9.59 ± 0.07	8.52 ± 0.01	ND	9.85 ± 0.07
BC-AEAPS$_{340}$	9.54 ± 0.05	8.16 ± 0.03	ND	7.02 ± 0.09
BC-AEAPS$_{280}$	9.77 ± 0.04	7.87 ± 0.04	ND	6.33 ± 0.24

ND: Not determined

4. Conclusion

In conclusion, we have developed a convenient method of grafting non-leachable bioactive amine functions onto the surface of bacterial cellulose nanofibrils, *vi*a a simple silylation treatment in water. Under a controlled set of conditions (never-dried material, water medium, room temperature, freeze-drying), water-leaching resistant (2-aminoethyl)-3-aminopropylsilyl functions were successfully introduced into BC, after reacting with the corresponding trimethoxysilane reagent (AEAPS). The success of the reaction was determined by i) the use of BC in its wet state, and ii) the use of sufficiently low initial concentrations of silane, to limit homocondensation and promote the reaction with hydroxylated substrate. The relatively good stability of the grafting was attributed to the structure of the AEAPS, which prevents the amine-catalyzed hydrolysis generally noted with

aminosilanes such as (3-aminopropyl)-trimethoxysilane (APS). The silylated material remained highly porous, hygroscopic and displayed sufficient thermal stability to support the sterilization treatments generally required in medical applications. The nanofibrillar structure and macro-porosity of the cellulose membranes was preserved after the silylation treatment, although a decrease in specific surface area was, attributed to a thickening of the fibrils after the silane condensation. After protonation of the amino sides by an acidic treatment, BC-$AEAPS_{280}$ was found to be an effective inherent antibacterial material against *S. aureus* in *in vitro* studies.

Further investigations would be interesting in order to understand better the impact of the concentration of aminosilanes in water on their condensation on BC nanofibrils. Further work on the mechanism responsible for the bioactivity by contact of protonated amino functions could help to give a better understanding of the critic parameters for the functionalization of BC with aminosilanes. Further study is also required to test the antibacterial properties of such materials against other microbial strains and in *in vivo* conditions. Finally, the heterogeneous functionalization of BC with accessible amine groups opens up a range of opportunities for the grafting of numerous compounds, such as peptides in order to target anti-bacterial activity against specific stains.

Supporting information

Figures supplied in the supporting information include size exclusion chromatographs of APS solution, TGA thermograms and nitrogen adsorption isotherms of unmodified and silylated-BC.

Acknowledgments

This work was developed within the scope of the European Joint Doctorate in Functional Materials Research EJD FunMat (Grant agreement ID: 641640) which funded G. Chantereau PhD fellowship. LCPO, CNRS UMR 5629 and CICECO-Aveiro Institute of Materials, POCI-01-0145-FEDER-007679 (FCT Ref. UID /CTM /50011/2013) financed by national funds through the FCT/MEC and when appropriate co-financed by FEDER under the PT2020 Partnership Agreement, are also acknowledged. C.S.R. Freire acknowledges FCT for her research contract under Stimulus of Scientific Employment 2017 (CEECIND/00464/2017).

References

Agarwal, A., McAnulty, J. F., Schurr, M. J., Murphy, C. J., & Abbott, N. L. (2011). Polymeric materials for chronic wound and burn dressings. *Advanced Wound Repair Therapies*, 186–208. https://doi.org/10.1533/9780857093301.2.186

ASTM D5373-16, Standard Test Methods for Determination of Carbon, Hydrogen and Nitrogen in Analysis Samples of Coal and Carbon in Analysis Samples of Coal and Coke. (2016). ASTM International.

Berlioz, S. (2007). *Etude de l'estérification de la cellulose par une synthèse sans solvant : Application aux matériaux nanocomposites.* Université Joseph-Fourier - Grenoble I. Retrieved from https://tel.archives-ouvertes.fr/tel-00266895v2

Berndt, S., Wesarg, F., Wiegand, C., Kralisch, D., & Müller, F. A. (2013). Antimicrobial porous hybrids consisting of bacterial nanocellulose and silver nanoparticles. *Cellulose*, *20*(2), 771–783. https://doi.org/10.1007/s10570-013-9870-1

Beveridge, T. J. (1999). Beveridge 1999, *181*(16), 1–9. Retrieved from papers2://publication/uuid/891DD90E-542E-4AE4-BFCA-1A88241FB325

Bieser, A. M., Thomann, Y., & Tiller, J. C. (2011). Contact-Active Antimicrobial and Potentially Self-Polishing Coatings Based on Cellulose. *Macromolecular*

494 *Bioscience*, *11*(1), 111–121. https://doi.org/10.1002/mabi.201000306
495 Bieser, A. M., & Tiller, J. C. (2011). Mechanistic Considerations on Contact-
496 Active Antimicrobial Surfaces with Controlled Functional Group Densities.
497 *Macromolecular Bioscience*, *11*(4), 526–534. https://doi.org/10.1002/mabi.201000398
498 Boswihi, S. S., & Udo, E. E. (2018). Methicillin-resistant Staphylococcus aureus :
499 An update on the epidemiology, treatment options and infection control. *Current*
500 *Medicine Research and Practice*, *8*(1), 18–24.
501 https://doi.org/10.1016/j.cmrp.2018.01.001
502 Chawla, P. R., Bajaj, I. B., Survase, S. a., & Singhal, R. S. (2009). Microbial
503 cellulose: Fermentative production and applications. *Food Technology and*
504 *Biotechnology*, *47*(2), 107–124.
505 Cheng, K.-C., Catchmark, J. M., & Demirci, A. (2009). Enhanced production of
506 bacterial cellulose by using a biofilm reactor and its material property analysis. *Journal*
507 *of Biological Engineering*, *3*(1), 12. https://doi.org/10.1186/1754-1611-3-12
508 Culler, S. R., Naviroj, S., Ishida, H., & Koenig, J. L. (1983). Analytical and
509 spectroscopic investigation of the interaction of CO2 with amine functional silane
510 coupling agents on glass fibers. *Journal of Colloid And Interface Science*, *96*(1), 69–79.
511 https://doi.org/10.1016/0021-9797(83)90009-7
512 Czaja, W. K., Young, D. J., Kawecki, M., & Brown, R. M. (2007). The future
513 prospects of microbial cellulose in biomedical applications. *Biomacromolecules*, *8*(1), 1–
514 12. https://doi.org/10.1021/bm060620d
515 Esa, F., Tasirin, S. M., & Rahman, N. A. (2014). Overview of Bacterial Cellulose
516 Production and Application. *Agriculture and Agricultural Science Procedia*, *2*, 113–119.
517 https://doi.org/10.1016/j.aaspro.2014.11.017
518 Etienne, M., & Walcarius, A. (2003). Analytical investigation of the chemical

519 reactivity and stability of aminopropyl-grafted silica in aqueous medium. *Talanta*, *59*(6),
520 1173–1188. https://doi.org/10.1016/S0039-9140(03)00024-9
521 Fernandes, S. C. M., Sadocco, P., Alonso-Varona, A., Palomares, T., Eceiza, A.,
522 Silvestre, A. J. D., … Freire, C. S. R. (2013). Bioinspired antimicrobial and
523 biocompatible bacterial cellulose membranes obtained by surface functionalization with
524 aminoalkyl groups. *ACS Applied Materials and Interfaces*, *5*, 3290–3297.
525 https://doi.org/10.1021/am400338n
526 Fernandes, S. C. M., Sadocco, P., Causio, J., Silvestre, A. J. D., Mondragon, I., &
527 Freire, C. S. R. (2014). Antimicrobial pullulan derivative prepared by grafting with 3-
528 aminopropyltrimethoxysilane: Characterization and ability to form transparent films.
529 *Food Hydrocolloids*, *35*, 247–252. https://doi.org/10.1016/j.foodhyd.2013.05.014
530 Fontana, J. D., De Souza, A. M., Fontana, C. K., Torriani, ! L, Moreschi, J. C.,
531 Gallotti, B. J., … Farah, L. F. X. (n.d.). *Acetobacter Cellulose Pellicle as a Temporary*
532 *Skin Substitute*. Retrieved from
533 https://link.springer.com/content/pdf/10.1007%2FBF02920250.pdf
534 Helander, I. M., Nurmiaho-Lassila, E. L., Ahvenainen, R., Rhoades, J., & Roller,
535 S. (2001). Chitosan disrupts the barrier properties of the outer membrane of Gram-
536 negative bacteria. *International Journal of Food Microbiology*, *71*(2–3), 235–244.
537 https://doi.org/10.1016/S0168-1605(01)00609-2
538 Hestrin, S., & Schramm, M. (1954). Synthesis of cellulose by Acetobacter
539 xylinum. Preparation of freeze-dried cells capable of polymerizing glucose to cellulose.
540 *Biochemical Journal*, *58*(2), 345–352.
541 Jorfi, M., & Foster, E. J. (2015). Recent advances in nanocellulose for biomedical
542 applications, *41719*, 1–19. https://doi.org/10.1002/app.41719
543 Lewis, K. (2001). Riddle of Biofilm Resistance. *American Society for*

Microbiology, *45*(4), 999–1007. https://doi.org/10.1128/AAC.45.4.999

Milović, N. M., Wang, J., Lewis, K., & Klibanov, A. M. (2005). Immobilized N-alkylated polyethylenimine avidly kills bacteria by rupturing cell membranes with no resistance developed. *Biotechnology and Bioengineering*, *90*(6), 715–722. https://doi.org/10.1002/bit.20454

Nguyen, V. T., Gidley, M. J., & Dykes, G. A. (2008). Potential of a nisin-containing bacterial cellulose film to inhibit Listeria monocytogenes on processed meats. *Food Microbiology*, *25*(3), 471–478. https://doi.org/10.1016/j.fm.2008.01.004

O'Neill, J. (2014). *Review on Antimicrobial Resistance. Antimicrobial Resistance: Tackling a Crisis for the Health and Wealth of Nations*. https://doi.org/10.1038/510015a

Saini, S., Belgacem, M. N., Salon, M. C. B., & Bras, J. (2016). Non leaching biomimetic antimicrobial surfaces via surface functionalisation of cellulose nanofibers with aminosilane. *Cellulose*, *23*(1), 795–810. https://doi.org/10.1007/s10570-015-0854-1

Serafica, G., Mormino, R., Oster, G. A., Lentz, K. E., & Koehler, K. P. (2003, April 30). *US10425978*. Retrieved from https://patents.google.com/patent/US7704523B2/en

Shan, B., Cai, Y. Z., Brooks, J. D., & Corke, H. (2007). Antibacterial properties and major bioactive components of cinnamon stick (Cinnamomum burmannii): Activity against foodborne pathogenic bacteria. *Journal of Agricultural and Food Chemistry*, *55*(14), 5484–5490. https://doi.org/10.1021/jf070424d

Shao, W., Wu, J., Liu, H., Ye, S., Jiang, L., & Liu, X. (2017). Novel bioactive surface functionalization of bacterial cellulose membrane. *Carbohydrate Polymers*, *178*(June), 270–276. https://doi.org/10.1016/j.carbpol.2017.09.045

Silva, N. H. C. S., Drumond, I., Almeida, I. F., Costa, P., Rosado, C. F., Neto, C. P., … Silvestre, A. J. D. (2014). Topical caffeine delivery using biocellulose membranes:

A potential innovative system for cellulite treatment. *Cellulose*, *21*(1), 665–674. https://doi.org/10.1007/s10570-013-0114-1

Silva, N. H. C. S., Rodrigues, A. F., Almeida, I. F., Costa, P. C., Rosado, C., Neto, C. P., … Freire, C. S. R. (2014). Bacterial cellulose membranes as transdermal delivery systems for diclofenac: In vitro dissolution and permeation studies. *Carbohydrate Polymers*, *106*, 264–269. https://doi.org/10.1016/j.carbpol.2014.02.014

Smith, E. A., & Chen, W. (2008). How to Prevent the Loss of Surface Functionality Derived from Aminosilanes. *Langmuir*, *24*(21), 12405–12409. https://doi.org/10.1021/la802234x.How

Taokaew, S., Phisalaphong, M., & Newby, B. min Z. (2015). Modification of bacterial cellulose with organosilanes to improve attachment and spreading of human fibroblasts. *Cellulose*, *22*(4), 2311–2324. https://doi.org/10.1007/s10570-015-0651-x

Thommes, M., Kaneko, K., Neimark, A. V., Olivier, J. P., Rodriguez-Reinoso, F., Rouquerol, J., & Sing, K. S. W. (2015). Physisorption of gases, with special reference to the evaluation of surface area and pore size distribution (IUPAC Technical Report). *Pure and Applied Chemistry*, *87*(9–10), 1051–1069. https://doi.org/10.1515/pac-2014-1117

Trovatti, E., Silva, N. H. C. S., Duarte, I. F., Rosado, C. F., Almeida, I. F., Costa, P., … Neto, C. P. (2011). Biocellulose membranes as supports for dermal release of lidocaine. *Biomacromolecules*, *12*(11), 4162–4168. https://doi.org/10.1021/bm201303r

Wippermann, J., Schumann, D., Klemm, D., Kosmehl, H., Salehi-Gelani, S., & Wahlers, T. (2009). Preliminary Results of Small Arterial Substitute Performed with a New Cylindrical Biomaterial Composed of Bacterial Cellulose. *European Journal of Vascular and Endovascular Surgery*, *37*(5), 592–596. https://doi.org/10.1016/j.ejvs.2009.01.007

Zhang, Z., Sèbe, G., Rentsch, D., Zimmermann, T., & Tingaut, P. (2014).

Ultralightweight and flexible silylated nanocellulose sponges for the selective removal of oil from water. *Chemistry of Materials*, *26*(8), 2659–2668. https://doi.org/10.1021/cm5004164

Zhang, Z., Tingaut, P., Rentsch, D., Zimmermann, T., & Sèbe, G. (2015). Controlled Silylation of Nanofibrillated Cellulose in Water: Reinforcement of a Model Polydimethylsiloxane Network. *ChemSusChem*, *8*(16), 2681–2690. https://doi.org/10.1002/cssc.201500525

Zhu, M., Lerum, M. Z., & Chen, W. (2012). How to prepare reproducible, homogeneous, and hydrolytically stable aminosilane-derived layers on silica. *Langmuir*, *28*(1), 416–423. https://doi.org/10.1021/la203638g

Zhu, X., Wu, H., Yang, J., Tong, J., Yi, J., Hu, Z., … Fan, L. (2015). Antibacterial activity of chitosan grafting nisin: Preparation and characterization. *Reactive and Functional Polymers*, *91–92*, 71–76. https://doi.org/10.1016/j.reactfunctpolym.2015.04.009